Quantifying the Influence of Cloud Seeding on Ice Particle Growth and Snowfall Through Idealized Microphysical Modeling

Ghazal Mehdizadeh * , Ehsan Erfani , Frank McDonough , Farnaz Hosseinpour

Posted Date: 29 October 2024

doi: 10.20944/preprints202410.2154.v1

Keywords: Weather Modification; Snow Growth Model; Aerosol-Cloud Interaction; Seeding-Induced Snowfall; Cloud Seeding; Cloud Microphysics; Ice Particle Growth

 doi:10.20944/preprints202410.2154.v1

Article

Quantifying the Influence of Cloud Seeding on Ice Particle Growth and Snowfall Through Idealized Microphysical Modeling

Ghazal Mehdizadeh [1,2,*], Ehsan Erfani [1,2], Frank McDonough [1,2] and Farnaz Hosseinpour [1,2]

[1] Division of Atmospheric Sciences, Desert Research Institute, Reno, NV, USA
[2] Atmospheric Sciences Graduate Program, University of Nevada, Reno, NV, USA
* Correspondence: ghazal.mehdizadeh@dri.edu

Abstract: Cloud seeding is a weather modification technique for enhancing precipitation in arid and semi-arid regions, including Western U.S. However, designing an optimal cloud seeding operation based on comprehensive evaluation metrics, such as seeding agent dispersion and atmospheric conditions, has yet to be thoroughly explored for this region. This study investigated the impacts of cloud seeding, particularly utilizing silver iodide, on ice particle growth within clouds through numerical modeling. By leveraging the Snow Growth Model for Rimed Snowfall (SGMR), the microphysical processes involved in cloud seeding across five distinct events were simulated. The events were in the Lake Tahoe region, nestled within the Sierra Nevada Mountain ranges in the western U.S. This model was executed based on six primary variables, including cloud top height, cloud base height, cloud top temperature, cloud base temperature, liquid water content, and ice water content. This study incorporated datasets from the Modern-Era Retrospective Analysis for Research and Applications Version 2 and the Clouds and the Earth Radiant Energy System. Findings revealed the importance of ice nucleation, aggregation, diffusion, and riming processes and highlighted the effectiveness of cloud seeding in enhancing ice particle number concentration, ice water content, and snowfall rates. However, event-specific analyses indicated diverse precipitation responses to cloud seeding based on initial atmospheric conditions. The SGMR modeling hints at the importance of improving ice microphysical processes and provides insights for future cloud seeding research using regional and global climate models.

Keywords: weather modification; snow growth model; aerosol-cloud interaction; seeding-induced snowfall; cloud seeding; cloud microphysics; ice particle growth

1. Introduction

Cloud seeding, a prevalent weather modification technique, involves introducing substances such as silver iodide (AgI) into clouds to change cloud particle properties and increase precipitation [1]. This method is particularly valuable in arid and semi-arid areas worldwide, where the growing population has a boosted demand for water [2]. Therefore, weather modification could reduce the effects of drought on human communities [2]. The change in precipitation as a result of cloud seeding has been shown by a number of studies. In observational studies by Manton et al. (2011) [3], a network of 13 ground generators and 44 precipitation gauges in the Snowy Mountains, Australia, showed a 14% increase in precipitation during 53 seeding periods compared to 31 unseeded instances. That study was later expanded [4] with 10 additional ground generators and 17 more gauges, enhancing the analysis. This expansion led to a 12% increase in precipitation in the southern target area at a 6% significance level and a 16% increase in the northern area at a 3% significance level. Further evidence comes from the 2014 Wyoming Weather Modification Pilot Project (WWMPP), which assessed the effect of AgI cloud seeding on snowfall through a randomized analysis of 118 seeding periods across the Medicine Bow ranges and the Sierra Madre in southeastern Wyoming [5]. Although results

 doi:10.20944/preprints202410.2154.v1

suggested a ~3% increase in precipitation, this was not statistically significant. To better understand the effects, simulations using the WRF model showed an average precipitation enhancement of 5%. Additionally, studies indicated that 27%-30% of winter precipitation occurs under conditions suitable for seeding [6], projecting an annual winter precipitation increase of about 1.5% [5]. Another significant study was conducted by Friedrich et al. (2020) [7] as part of the Seeded and Natural Orographic Wintertime Clouds: the Idaho Experiment (SNOWIE) project. In this study, AgI was dispersed from an aircraft upwind of the Payette River basin. The flights were conducted in areas with minimal natural precipitation, enabling accurate identification and monitoring of radar echo patterns and the corresponding increases in ground precipitation due to cloud seeding. The observed enhancements in snowfall rate during seeding varied from approximately 0.4 mm/hr to 1.2 mm/hr [7].

The idea of artificially enhancing precipitation is appealing to water resource managers, as it could contribute to balancing and sustaining water supply and demand year-round [2,8,9]. Significant amounts of freshwater are introduced into Earth's hydrological cycle as precipitation from clouds [2,10]. Between 1950 and 2010, the population of the United States more than doubled, transitioning from rural to urban regions [11]. The population grew most in the southern and western states [12]. Communities in the western states facing water shortages and increasing demands turned to weather modification techniques in order to expand their water resources [12]. Research indicates that in the coming decades, water is expected to become a scarcer resource due to the ever-increasing population and climate change, endangering snow reservoirs across the western mountains [12,13].

Two primary techniques exist for cloud seeding: hygroscopic and glaciogenic seeding. Hygroscopic seeding accelerates the coalescence of droplets within liquid clouds to form larger, precipitation-ready droplets. This method typically involves distributing salts varying in size from 0.1 to 10 μm at the cloud base [14,15]. In contrast, glaciogenic seeding aims to induce ice formation within clouds containing supercooled liquid water (SLW) [16]. This technique often employs ice-forming agents, such as AgI or dry ice, to facilitate the heterogeneous nucleation of ice. Glaciogenic seeding is commonly applied to convective or winter orographic clouds [12]. In convective clouds formed by surface heating, the interplay between dynamics and microphysics presents various possibilities to enhance precipitation [15]. In glaciogenic seeding, seeding agents are introduced into clouds to increase the concentration of ice-nucleating particles (INP) as well as enhance the cloud's buoyancy through the release of latent heat from SLW freezing. Both effects are anticipated to happen simultaneously because the formation of ice particles leads to latent heat release [15,17,18].

Precipitation in wintertime orographic clouds is affected by regional orography, with SLW forming as moist air ascends over mountain ranges [15,19]. Orographic cloud seeding involves introducing INP into the SLW to generate ice particles at temperatures of about −5°C, which grow through collision and deposition [15,20]. The effects of ground-based seeding of AgI on the orographic cloud microphysics were examined by Geerts et al. (2010) [21] as part of the Wyoming Weather Modification Pilot Project (WWMPP) [22]. By comparing radar data from seeded and unseeded flights utilizing contoured frequency by altitude displays (CFADs), they identified increased seeding impact with higher Froude numbers, indicating reduced flow stability. Further, a record of precipitation enhancement processes in wintertime orographic clouds over southwestern Idaho was provided by French et al. (2018) [20]. They outline two aircraft seeding methods with AgI, consisting of burn-in-place, where INP is released horizontally from the aircraft at effective seeding heights, and ejectable flares, deployed at or above the supercooled water level, suitable for mountainous areas but with risks of burnout. Ground-based seeding strategies, such as acetone burners, artillery shells, and rockets [23], face challenges in assuring that INP arrives at the right cloud level. Remote sensing can track seeded material, and modeling and Observation analyses indicate direct seeding is more influential than ground-based methods [24,25].

Previous studies have primarily focused on employing seeding to enhance precipitation [5,12,20] or for hail damage mitigation [26,27]. Observational studies provide real-world data to validate models and offer detailed insights into cloud seeding processes, which are essential for directing future research and improving weather modification techniques. However, while numerous

 doi:10.20944/preprints202410.2154.v1

observational studies [3,5,28] have attempted to investigate the effects of cloud seeding on seasonal precipitation levels, their estimation through statistical analyses and observations presents notable challenges. First, there is the issue of identifying the location and timing of the seeded clouds within the natural clouds (absence of natural control). Second, the complexity of identifying seeding effects and detecting an increase in surface precipitation [29]. Third, the cost of long-term seeding experimentations [30]. Therefore, advancements in numerical models that simulate the physics of cloud seeding and cloud processes, validated by observational data, are proving crucial [12].

Numerical models are valuable for effectively evaluating and quantifying the effects of cloud seeding [12]. Xue et al. (2013) [25] showed different outcomes from ground-based versus aircraft seeding in the Payette and Snake River basins, Idaho. Further, they utilized the 2D Weather Research and Forecasting (WRF) model integrated with a prognostic aerosol model with cloud seeding parameters. The study revealed significant spatial variability in precipitation, with increases up to 2 mm in some areas, but most regions experienced less than 1 mm of additional precipitation. This indicates that localized measurements may not represent conditions across the entire area [25]. Similarly, four cloud-seeding cases in the same area, conducted during a snow trace chemistry field campaign from 2003 to 2005, were simulated by Xue et al. (2017) [31]. Using the WRF Model in large-eddy simulation mode with a 667 m grid spacing, two airborne and two ground-based events were examined. The results, compared with soundings, Snowpack Telemetry (SNOTEL) site precipitation, and silver concentrations in snow samples, showed that the simulated concentrations matched the observed data's magnitude and spatial distribution [31]. Furthermore, large eddy simulation models have been utilized in numerous studies [e.g.,32,33] to explore AgI seeding in orographic clouds. Their findings suggest that a limitation of practical seeding is the vertical distribution of seeding agents and their efficiency in reaching the clouds, and therefore cloud dynamics is not greatly influenced by seeding. Although numerical model simulations offer insights into the influence of seeding, it is essential to validate them in the real atmosphere. Regional climate simulations with a resolution of 6 km or lower [13,34,35] have indicated that modern mesoscale models, using the latest microphysical schemes, can simulate natural precipitation in complex terrains during the cold season and it is possible to simulate seasonal snowfall with an accuracy that approaches within 10% of observations. Before this advancement, model uncertainty hindered scientists from using cutting-edge models for orographic cloud seeding [12]. Following these achievements, models are now being used to assess orographic cloud seeding projects [5].

Despite these advantages, mesoscale models are analytically and computationally expensive. The Snow Growth Model (SGM) [36] was designed to study snow and ice microphysical processes with great accuracy and computational efficiency. This model proves especially advantageous since satellite measurements of cloud properties are not available or reliable at the bottom of clouds, offering a dependable method for the growth of snow and ice from the cloud top to the cloud bottom using main microphysical processes. Building on prior research [37,38], this study contains substantial enhancements to the SGM, including the incorporation of the riming process and ice heterogeneous nucleation. With these updates, the model was termed the Snow Growth Model for Rimed Snowfall (SGMR).

This study suggests an innovative application of the SGMR for cloud seeding in various background conditions, enhancing our comprehension of ice nucleation and the development of ice growth throughout the cloud. Section two describes the methodology used in this study. Section three discusses the results, including atmospheric conditions and model outputs. Finally, the Conclusions are presented in Section four.

2. Data and Methodology

2.1. Datasets

The Modern-Era Retrospective Analysis for Research and Applications, Version 2 (MERRA-2) [39], is used here to investigate meteorological variables. MERRA-2 is NASA's atmospheric reanalysis from 1980 to the present, utilizing an advanced version of the Goddard Earth Observing System

 doi:10.20944/preprints202410.2154.v1

Model, Version 5 (GEOS-5) [40] data assimilation system. All datasets from MERRA-2 are distributed on a constant horizontal grid, featuring 576 longitudinal points and 361 latitudinal points. This design corresponds to a grid resolution of 0.625° longitude by 0.5° latitude. Additionally, the data are structured across 72 model layers [41], enabling detailed atmospheric analysis.

Moreover, the Clouds and the Earth Radiant Energy System (CERES) [42] is employed to collect cloud variables. CERES is designed for the Earth Observing System (EOS) [42–44], and encompasses solar and terrestrial radiation fluxes as well as various ice and liquid cloud properties at specific vertical levels. It is a global dataset, and its spatial coverage relies on the satellite orbit, varying from about 20 km at nadir for Single Scanner Footprint (SSF) products to 1 degree by 1 degree (latitude by longitude) for gridded daily and monthly averages. We used 1-degree gridded daily data in this study. CERES cloud characteristics are specified through concurrent measurements from different EOS tools, such as the Moderate Resolution Imaging Spectroradiometer (MODIS) [45]. MODIS, on NASA's Terra and Aqua satellites, has been used to retrieve global cloud and aerosol properties and atmospheric conditions [46]. In this study, the model is driven using MERRA-2 and CERES datasets.

2.2. Snow Growth Model for Rimed Snowfall

The Snow Growth Model for Rimed Snowfall (SGMR) is a one-dimensional, analytically based microphysical model that is computationally efficient, making it a cost-effective option for modeling processes involved in the growth of ice and snow particles. It is particularly valuable in situations where observational data at the surface or cloud base is either unavailable or uncertain, providing a reliable means of simulating snow growth even in the absence of direct measurements.

The Snow Growth Model (SGM) [36] was initially developed as a process-based model to simulate aggregation and vapor deposition processes, disregarding the impacts of updraft and riming due to relatively weak updrafts and low supercooled liquid water content (LWC). This is specific to mid-latitude cyclones in continental areas of the United States during the winter season.

Over time, progress was made to improve microphysical processes [37] by incorporating the riming process [38,47] to upgrade vapor diffusional mass growth rate, ice particle mass-dimension, project area-dimension, and fall speed-dimension relationships. These improvements were highlighted by integrating the riming process into the model, which led to its updated designation as the snow growth model for rimed snowfall (SGMR).

The SGMR in this study has been further developed to include the nucleation process, crucial for accurately simulating the effects of cloud seeding. By incorporating nucleation, the SGMR can more reliably simulate how substances (e.g. silver iodide) used in cloud seeding, affect precipitation. Within the SGMR, ice nucleation for four heterogeneous nucleation processes (covers condensation, deposition, contact, and immersion processes) has been implemented within the temperature range of -40°C to 0°C, following the formulations from Liu et al. (2007) [48]. Within the seeding plume, an AgI mean radius of 50 nanometers is assumed [25], with an AgI number concentration of 700 cm^{-3} [49], and the plume extends to the lowest 800 m of the cloud. Another assumption in the model is that in case the IWC exceeds 0.05 g/m^3 at the top of the cloud, the model will select this threshold value (Table 1). Based on previous studies [50,51], this approach is expected to yield a mean diameter smaller than 3000 microns within the cloud layer, keeping it within a physical range.

The process of ice particle growth within clouds involves several mechanisms, each playing an integral role in shaping precipitation. These processes are illustrated in the conceptual model as indicated in Figure 1. The mechanisms include vapor deposition, where water vapor condenses onto ice nuclei, aggregation, which involves the collision and merging of ice crystals, riming, where supercooled water droplets freeze upon contact with ice crystals, and ice nucleation. These fundamental microphysical processes are integrated into the SGMR to enable the simulation of ice microphysics.

 doi:10.20944/preprints202410.2154.v1

Table 1. Model Inputs for Five Cloud Seeding Events in the Tahoe Region.

Event	Date	Cloud Top Height (km)	Cloud Base Height (km)	Cloud Top Temperature (°C)	Cloud Base Temperature (°C)	LWC (g/m³)	IWC (g/m³)
1	March 6, 2021	4.929	3.309	-19	-9	0.158	0.049
2	December 16, 2021	3.87	2.019	-13	-3	0.249	0.05
3	March 5, 2022	5.013	2.249	-23	-8	0.102	0.05
4	April 16, 2022	3.996	2.486	-11	-4	0.16	0.05
5	March 9, 2021	4.1	2.22	-21	-6	0.2	0.05

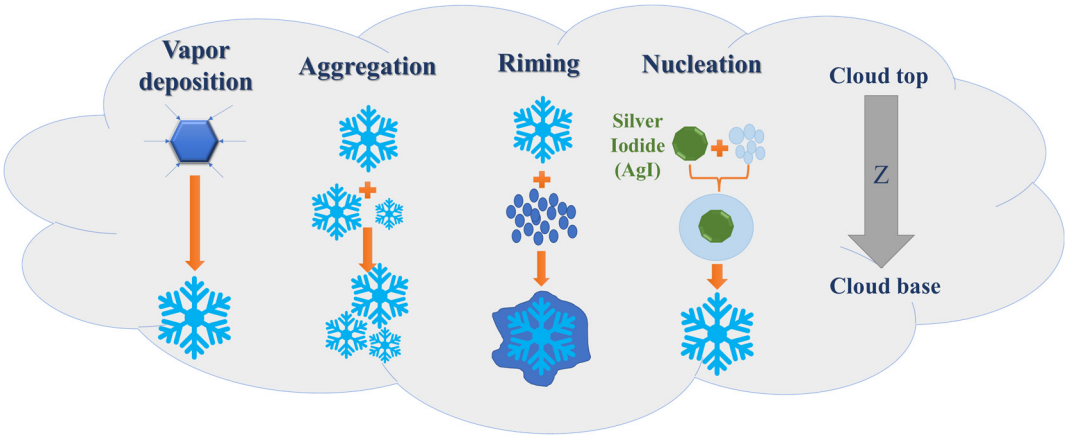

Figure 1. Conceptual model illustrating the Ice particle growth mechanism through clouds integrated into the SGMR. The model demonstrates how snowfall microphysics are simulated, including vapor deposition, aggregation, riming, and ice nucleation mechanisms.

SGMR uses inputs from a comprehensive array of variables including cloud top and base height, temperature, maximum LWC in the cloud layer, and ice water content (IWC) near the top cloud. Subsequently, the model simulates the growth behavior of ice particles in response to forcing data. The model runs both with and without considering cloud seeding, a critical factor in our study. This approach aims to evaluate how cloud seeding influences various parameters (a) number concentration, referring to the number of ice particles present per volume of air, (b) IWC, representing the mass mixing ratio of ice per volume of air, (c) mass-weighted terminal fall speed, which denotes the velocity at which ice particles descend within the cloud, and (d) snowfall rate, which is the vertical flux of IWC or IWC multiplied by fall speed indicating the rate at which snow falls from the atmosphere.

Figure 2 showcases the geographical locations of cloud-seeding ground-based generators in the Lake Tahoe region across five locations, ranging in elevation between 1500 to 2500 meters. The specific generator sites are Cisco, Ward, Barker, Bunker, and Morattini, operated by the Desert Research Institute (DRI). These generators are strategically positioned to optimize the cloud-seeding process and enhance precipitation levels in targeted areas. Cloud seeding operations are conducted during the winter season, specifically from November to May.

 doi:10.20944/preprints202410.2154.v1

Figure 2. Cloud Seeding Generator Locations in the Lake Tahoe Region.

The SGMR model is applied to analyze five distinct cloud seeding occurrences in the Tahoe region on March 6, 2021, December 16, 2021, March 5, 2022, April 16, 2022, and March 9, 2021 (Table 1). The required model inputs are sourced from CERES satellite and MERRA-2 reanalysis datasets. Model inputs include cloud top and base heights (km), cloud top and cloud base temperatures (°C), liquid water content (LWC), and ice water content (IWC) measured (g/m^3). Table 1 illustrates the specific model inputs utilized for five seeding events in the Tahoe area.

3. Results and Discussion

This section presents the findings of our study on the cloud seeding mechanism. The main objective was to simulate the growth behavior of ice particles within clouds. The variations in cloud top and base heights, temperatures, LWC, and IWC across five events as presented in Table 1, provide insights into the differing microphysical properties of the clouds. The vertical extent of the cloud layers during each event was determined by measuring the cloud's top and base heights. On March 6, 2021, the cloud top was at 4.929 km, and the base was at 3.309 km, indicating a relatively thick cloud layer (thickness of 1.62 km). On the second event (December 16, 2021), the cloud top was at 3.870 km, with a base at 2.019 km, suggesting a thicker yet lower cloud. The event on March 5, 2022, showed cloud top and base heights of 5.013 and 2.249 km, respectively.

Furthermore, on April 16, 2022, the cloud thickness was 1.51 km, nearly similar to Event 1. The cloud top at 4.1 km and the base at 2.22 km presented a relatively thick layer in the last event, on March 9, 2021. The temperatures at the cloud tops ranged from -23°C to -11°C. The coldest cloud tops were on March 5, 2022, where the cloud had the highest altitude among all events, and the warmest was on April 16, 2022. The temperatures at the cloud bases varied from -9°C to -3°C. The coldest base temperature was observed on March 6, 2021, and the warmest on December 16, 2021. The values of temperature within the cloud layer are critical for determining various processes and properties such as vapor deposition, nucleation, and viscosity.

Additionally, LWC and IWC measurements indicate the amounts of supercooled cloud droplets and ice particles in the clouds. LWC showed considerable variability, with values ranging from 0.102

 doi:10.20944/preprints202410.2154.v1

g/m³ to 0.249 g/m³. The highest amount was observed on December 16, 2021, while the lowest was on March 5, 2022. These differences in cloud properties are crucial for understanding cloud behavior and are significant for weather modification and atmospheric research applications. The values of IWC at the cloud top are important to determine the change in most ice microphysical variables within the cloud layer. The values of LWC affect the effectiveness of the riming process.

3.1. Atmospheric Condition

The atmospheric conditions (depicted in Figure 3) of these five events were also monitored at the weather stations [52] nearest to the ground-based generators. At the first event, the average temperature was -3°C, with a maximum of 0°C and a minimum of -6°C, at Bunker Station, which is situated at an elevation of 2,293 meters. Following this, data from the Northstar weather station, positioned at an elevation of 2,625 meters, on December 16, 2021, indicated that the average air temperature was -7°C, with variations between a high of -6 and a low of -9°C. Wind speeds averaged 13 km/h, with occasional peaks reaching 58 km/h, mainly from the west-southwest (259 degrees). Subsequently, for Event 3 on March 5, 2022, wind speed averaged 15 km/h, peaking at 69 km/h, predominantly from the northeast at 67 degrees at Ward station, located at an elevation of 2,597 meters. In contrast, during event four in the Northstar Weather Station, the air temperature averaged -2°C, ranging from -1°C to -4°C. Wind speeds were more pronounced, averaging 23 km/h and peaking at 70 km/h, mostly from the southwest (209 degrees). Lastly, on March 9, 2021, the westerly winds were notably strong, averaging 40 km/h, with gusts reaching 68 km/h at the elevation of 2,597m at Ward Station. These conditions coincided with cool temperatures averaging -8°C, ranging between -7°C and -8°C. During the observed events, the conditions indicated consistently high humidity levels, with relative humidity ranging from 94% to 100%. The dew point and wet bulb temperatures fluctuated within the range of -11°C to -2°C, suggesting persistently cool and moist conditions conducive to seeding activities.

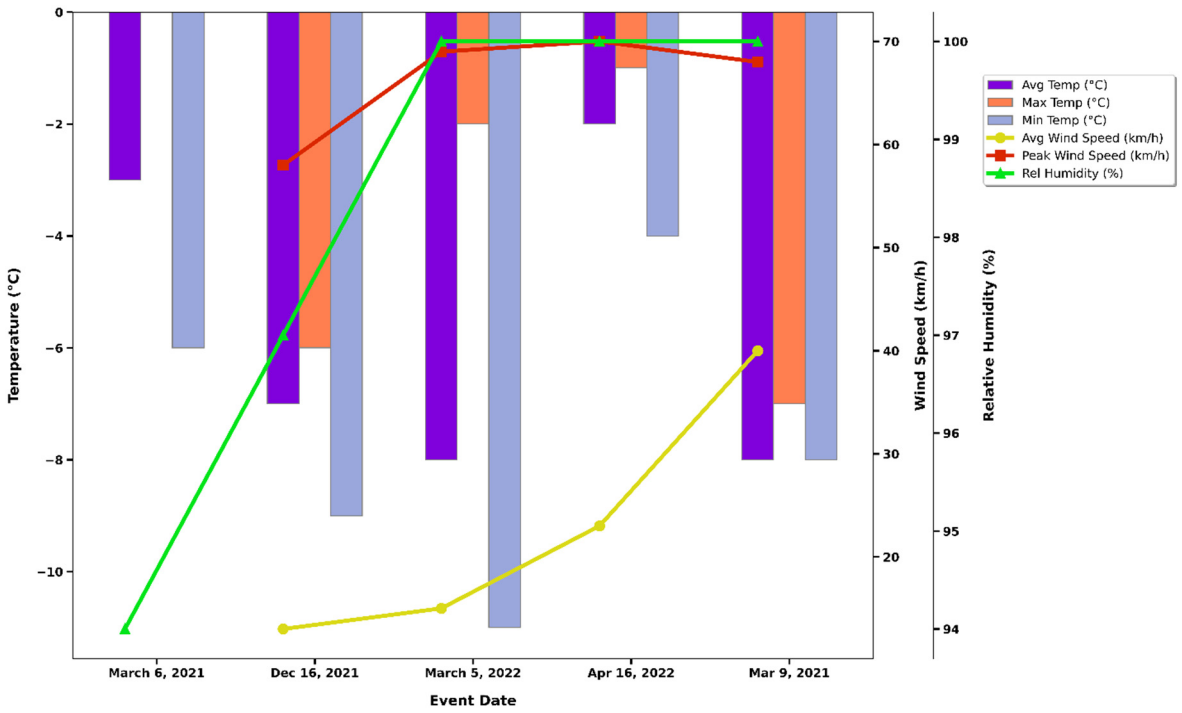

Figure 3. Combined atmospheric conditions on Event 1 (March 6, 2021), Event 2 (December 16, 2021), Event 3 (March 5, 2022), Event 4 (April 16, 2022), and Event 5 (March 9, 2021), showing average temperature (°C), maximum temperature (°C), and minimum temperature (°C), average wind speed (km/h), peak wind speed (km/h), and relative humidity (%). Data sourced from weather stations closest to the ground-based generators, as provided by the Western Regional Climate Center.

 doi:10.20944/preprints202410.2154.v1

3.2. Model Results

By running the model under varied scenarios, the effects of cloud seeding on snow particle formation and dynamics can be effectively identified. In the absence of seeding, snow particles form naturally around atmospheric aerosols without the introduction of nucleating agents. Regarding Event 1 on March 6, 2021, Figure 4 (right panels) shows that the number concentration of particles decreases from 14 Liter^-1 at the cloud top to 2 Liter^-1 at the bottom in natural conditions for the run with all 3 processes. This reduction is attributed to the growth of cloud particles from the top to the bottom of the cloud, where larger or heavier particles are more efficiently removed. The figure also highlights that aggregation plays a more significant role than riming in reducing the number of ice particles. Conversely, the snowfall rate, as depicted in Figure 5 (right panels), increases by approximately 0.2 mm/hr when three processes of riming, aggregation, and diffusion occur simultaneously. The vertical profile of IWC in Figure 6 (right panels) indicates an increase from the cloud top to the bottom (from 0.05 to 0.075 gr/cm3), driven by the phase transition from vapor to ice and the accumulation of cloud droplets on ice surfaces through riming. Although aggregation does not change the IWC, riming notably enhances it. Furthermore, Figure 7 (right panels) illustrates an increase in fall speed in scenarios that include all ice particle growth mechanisms, where the fall speed enhances from the cloud top to the base due to the increase in particle size and mass per area ratio.

When seeding is active, the first significant effect observed is an increase in the number concentration of ice particles. This rise is primarily due to the AgI plume effect at the lower part of the cloud, where nucleation significantly enhances the number of ice particles (Figure 4; left panels). In Event 1, this concentration peaks at 38 particles per liter at an altitude of 3600 meters. Seeding also notably enhances snowfall rates by forming a greater number of ice particles, especially evident in scenarios involving riming, as shown in Figure 5 (left panels). In this event, the snowfall rate increase was 0.17 mm/hr, as the newly formed ice particles substantially boosted the IWC. This increase aligns with simulated transitions in other parameters, starting at altitudes around 4000 meters. While aggregation produces larger but less dense snowflakes, riming significantly raises the ice mass through the accumulation of cloud droplets by ice particles. Additionally, cloud seeding considerably enhances the IWC, as depicted in Figure 6 (left panels). Comparative analysis of conditions with and without seeding shows that riming at the cloud base in Event 1 results in a 0.04 g/cm^3 increase in IWC. Furthermore, the introduction of nucleating agents alters the physical characteristics of snowflakes, including their size and shape, which affects their fall speed. Despite this, the overall impact on the mass-weighted fall speed is minimal because the nucleated ice particles are small.

In the natural conditions of Event 2, the cloud processes exhibit a typical, gradual transition in all measured parameters. The number concentration of ice particles for the run with the inclusion of diffusion, aggregation, and riming shows a consistent decrease with altitude, beginning to reduce from about 8 particles per liter at 3800 meters. The snowfall rate under unseeded conditions reaches the maximum of 0.45 mm/h at the cloud base. The IWC increases from top to bottom, reaching a maximum of 0.09 gr/cm^3 at the cloud base, reflective of higher ice content in comparison to Event 1, in natural cloud conditions. Similarly, the fall speed exhibits a maximum speed of about 135 cm/s at 2000 meters.

Upon introducing seeding in Event 2, the cloud microphysics are significantly altered. The number concentration when diffusion, aggregation, and riming are included, surges to 10 particles per liter at 2500 meters, an increase that highlights the effectiveness of nucleating agents in stimulating ice particle formation. Likewise, the snowfall rate sees a considerable increase, reaching 0.6 mm/h at the cloud base, which is 0.15 mm/hr higher than the unseeded condition. The IWC reaches a higher peak of 0.12 gr/cm^3 at 3000 meters, a clear indication of a more efficient riming process facilitated by the seeding. Moreover, the fall speed of the particles increased in the scenario consisting of all mechanisms.

 doi:10.20944/preprints202410.2154.v1

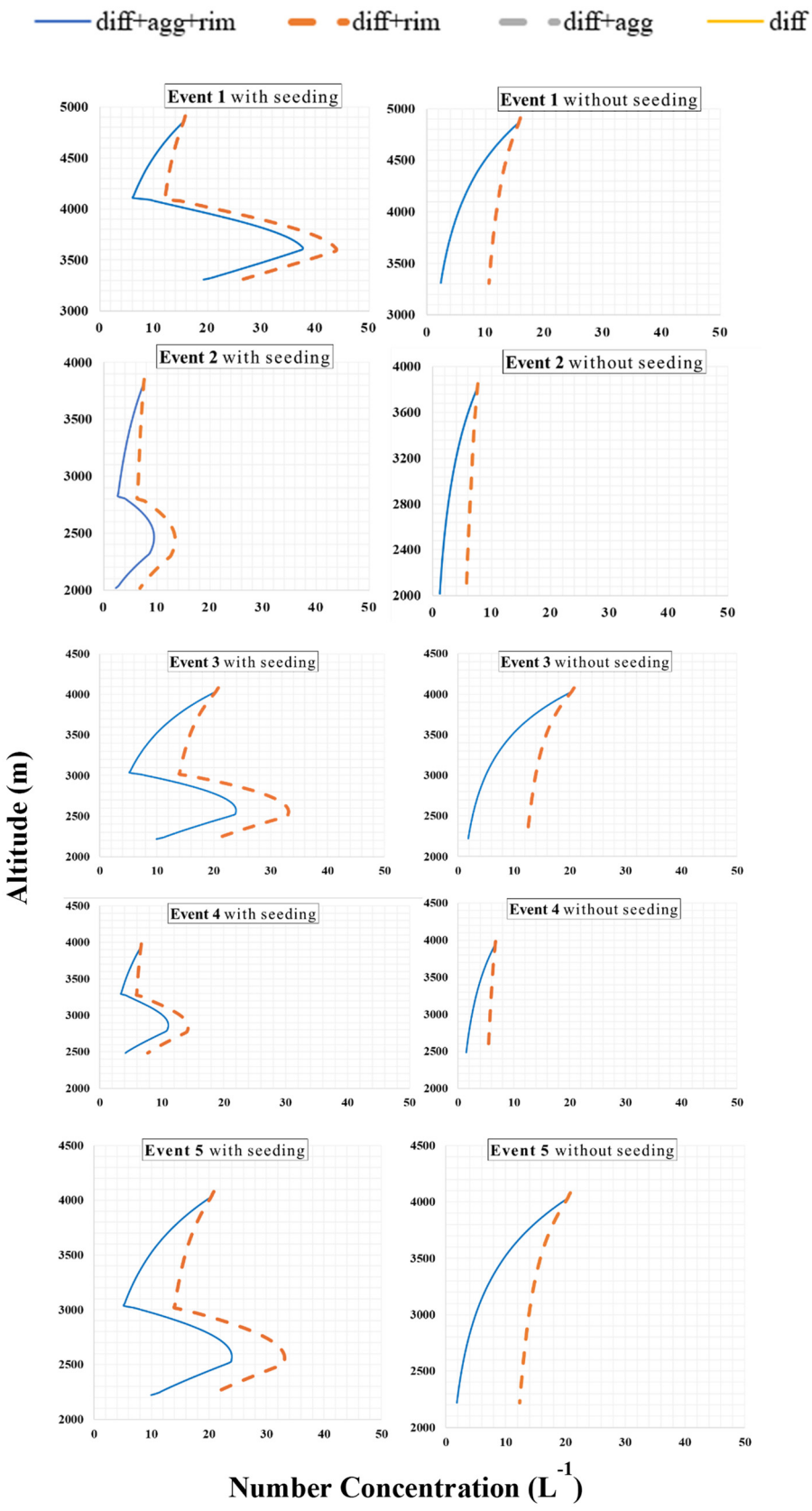

Figure 4. Comparison of the effects of seeding on Event 1 (March 6, 2021), Event 2 (December 16, 2021), Event 3 (March 5, 2022), Event 4 (April 16, 2022), and Event 5 (March 9, 2021) across four scenarios incorporating Diffusion, Aggregation, and Riming. The analysis includes changes in Number concentration.

 doi:10.20944/preprints202410.2154.v1

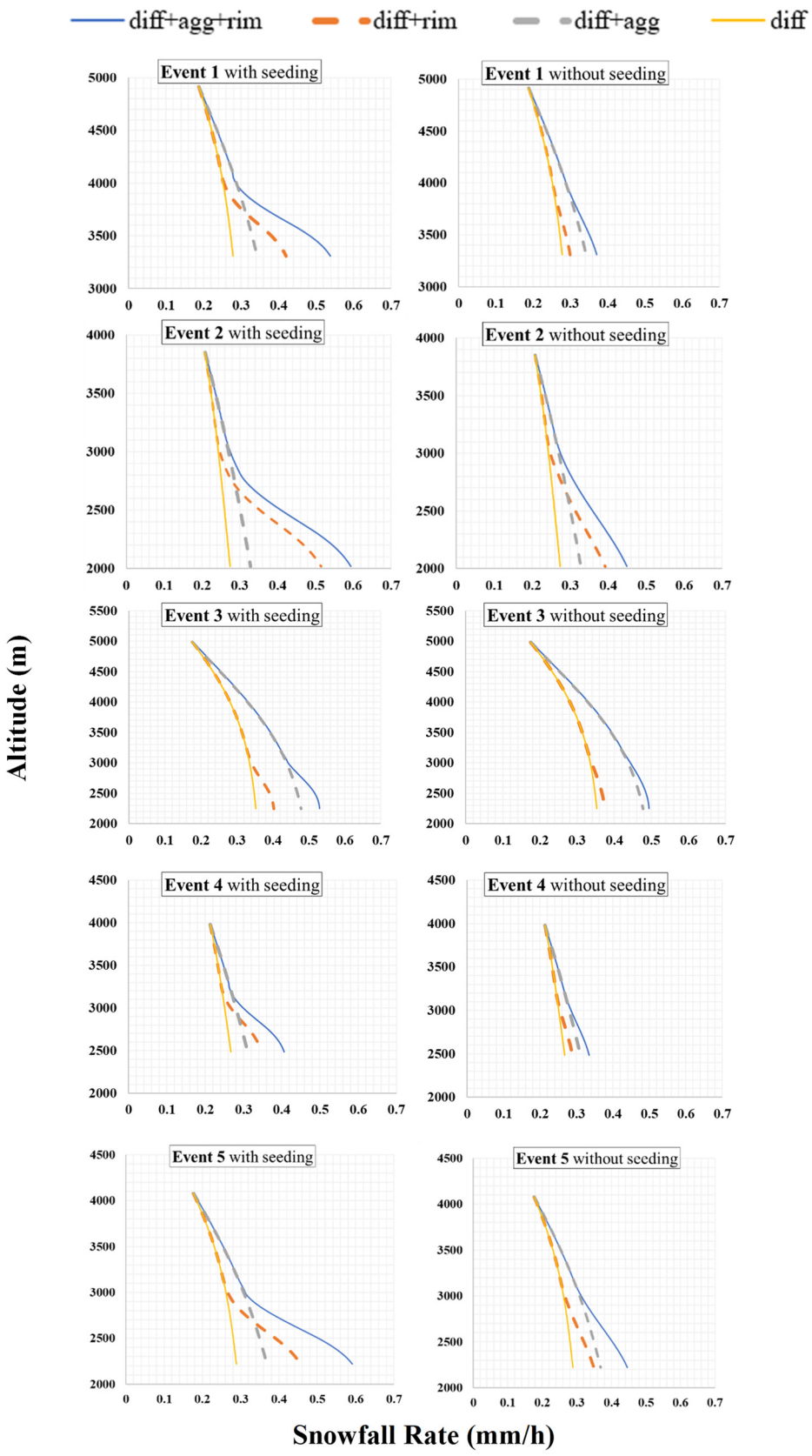

Figure 5. Comparison of the effects of seeding on Event 1 (March 6, 2021), Event 2 (December 16, 2021), Event 3 (March 5, 2022), Event 4 (April 16, 2022), and Event 5 (March 9, 2021) across four scenarios incorporating Diffusion, Aggregation, and Riming. The analysis includes changes in Snowfall rate.

 doi:10.20944/preprints202410.2154.v1

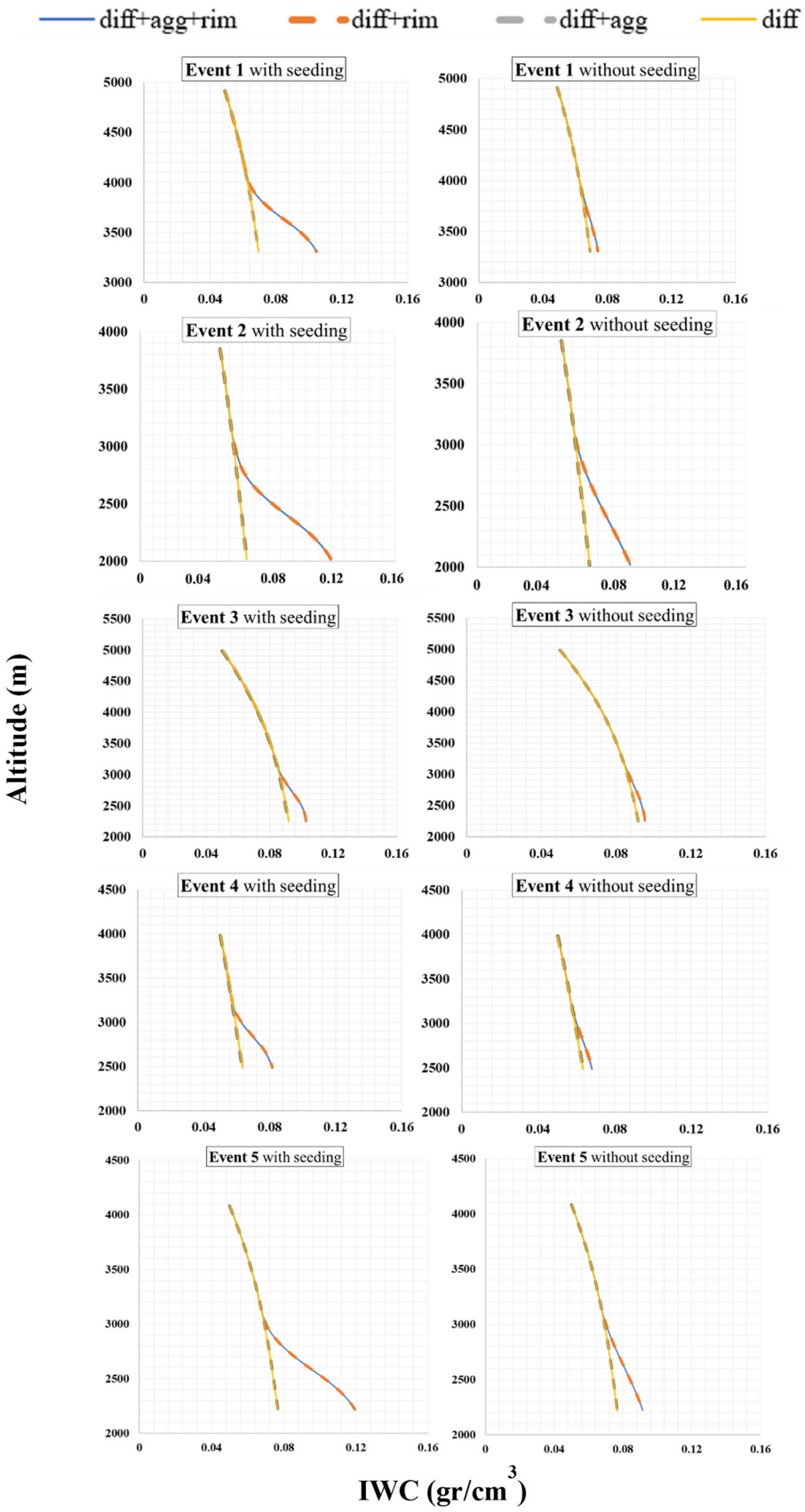

Figure 6. Comparison of the effects of seeding on Event 1 (March 6, 2021), Event 2 (December 16, 2021), Event 3 (March 5, 2022), Event 4 (April 16, 2022), and Event 5 (March 9, 2021) across four scenarios incorporating Diffusion, Aggregation, and Riming. The analysis includes changes in IWC.

 doi:10.20944/preprints202410.2154.v1

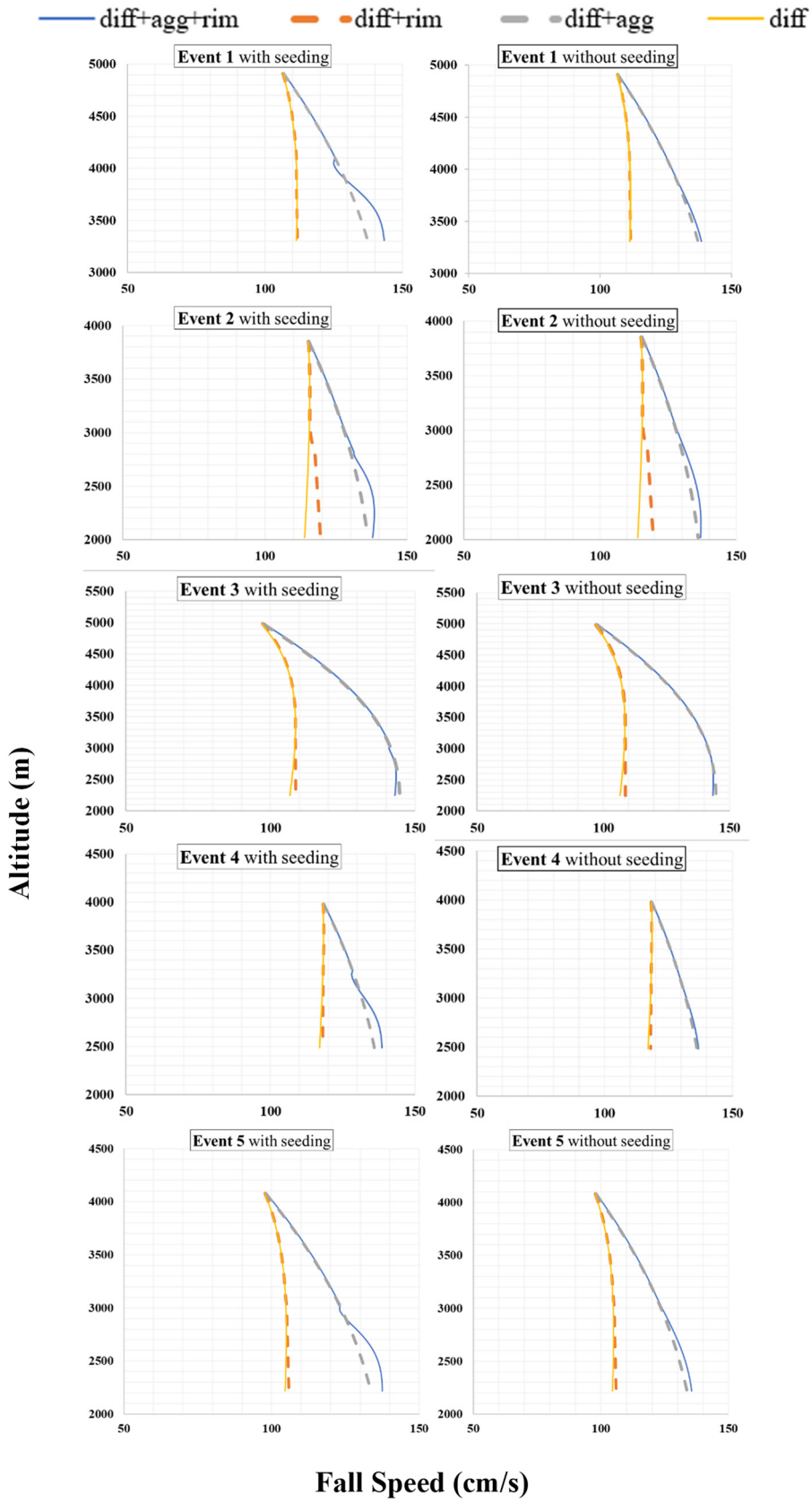

Figure 7. Comparison of the effects of seeding on Event 1 (March 6, 2021), Event 2 (December 16, 2021), Event 3 (March 5, 2022), Event 4 (April 16, 2022), and Event 5 (March 9, 2021) across four scenarios incorporating Diffusion, Aggregation, and Riming. The analysis includes changes in Fall speed.

 doi:10.20944/preprints202410.2154.v1

The model outcomes for event 3 (on March 5, 2022), indicate that the number concentration of ice particles significantly reduces from 21 to about 12 particles per liter when riming and diffusion are present. In scenarios involving all three processes, the number concentration at the cloud base further drops to approximately 2 particles per liter, because aggregation causes ice particles to stick together. Moreover, the snowfall rate increases from 0.17 mm/hr at an altitude of 5013 meters to about 0.5 mm/hr at 2249 meters, reflecting enhanced snow formation as particles descend. While the IWC shows minimal changes across all scenarios, it consistently enhances from top to bottom of the cloud. Also, the fall speed of particles rises from 95 cm/s at the cloud top to 110 cm/s at the cloud base in scenarios with aggregation and aggregation+diffusion, and to approximately 145 cm/s when aggregation is not present, highlighting the impact of particle growth mechanisms on fall velocity.

In contrast, the seeded condition of Event 3 results in the number concentration of ice particles reaching 24 particles per liter, when three processes are present. Although Event 3 features the lowest cloud top temperature and the highest altitude among all events, its number concentration remains lower than that simulated in Event 1. Furthermore, the snowfall rate grows at the 2500-meter level, indicating enhanced precipitation efficiency due to seeding. A modest increase of about 0.01 g/cm^3 in IWC near the cloud base is observed, marking the lowest increase among all events. Additionally, the fall speed of particles shows negligible change with seeding, suggesting that while nucleation enhances ice particle formation, it does not greatly affect their falling rate.

During Event 4 on April 16, 2022, the cloud's vertical depth was notably shallower compared to other observed events, with a measured depth of 1.51 km (Table 1). Under the unseeded condition, the number concentration decreased minimally, reaching approximately 2 particles per liter at the cloud bottom. The snowfall rate increased to 0.33 mm/hr at the cloud base, located at an altitude of 2486 meters. Additionally, there was only a minimal increase in IWC near the cloud base, indicating limited growth in ice mass under natural conditions. The overall trend in fall speed was a moderate increase with decreasing height, from 120 cm/s at the cloud top to approximately 135 cm/s at the base. This trend suggests that as ice particles descended, their size and mass contributed to a greater fall speed.

Following the injection of cloud seeding, significant changes in cloud microphysics were observed in Event 4. The number concentration of ice particles increased to 9 particles per liter at an altitude of 2800 meters, 300 meters above the cloud base. The snowfall rate began to rise from the middle of the cloud at approximately 2800 meters and reached 0.41 mm/hr at the cloud base, indicating a 0.05 mm/hr increase due to seeding. The IWC also increased by about 0.01 gr/cm^3 after seeding, reflecting enhanced ice particle formation and growth. Furthermore, seeding led to an increase in the mass-weighted fall speed.

Regarding the last event on March 9, 2021, the number concentration of ice particles under natural atmospheric conditions decreased from 21 particles per liter at the cloud top to 2 particles per liter at the cloud base for run with the inclusion of three processes of diffusion, aggregation, and riming. Moreover, the snowfall rate increases, predominantly influenced by aggregation near the cloud top and by riming near the cloud bottom. The riming process is much stronger towards the cloud bottom because LWC values are higher in this part of the cloud. As a result of the collection of cloud droplets by ice particles, dense rimed particles form, and this enhances the overall IWC and therefore snowfall rate in simulations with the inclusion of riming. Since riming is negligible near the cloud top, aggregation dominates and as a result, the snowfall rate is stronger in simulations including the aggregation process. Although aggregation did not alter the IWC, riming notably enhanced it. Specifically, the difference in IWC between scenarios including riming and those without was approximately 0.015 g/cm^3 at the cloud base. Furthermore, an increase in fall speed was shown in scenarios encompassing all ice particle growth mechanisms.

When seeding was active, the number concentration began to increase and reached a value of 24 Liter^-1 at an altitude of around 3000 meters due to the plume effect at the lower part of the cloud. Here, nucleation significantly enhanced the number of ice particles. Additionally, seeding led to a notable enhancement in snowfall rates by forming a greater number of snowflakes in scenarios

 doi:10.20944/preprints202410.2154.v1

involving riming. This enhancement amounted to approximately 0.14 mm/hr. Moreover, in scenarios that included riming, the IWC increased by 0.025 g/cm³.

In summary, SGMR findings indicate that riming has a significant impact due to the collection of cloud droplets by ice particles that leads to enhancing their mass and area while making negligible change in their size. Notably, seeding increased the snowfall rate, with scenarios involving cloud seeding resulting in a snowfall rate on average 24% higher than those with no cloud seeding. The lowest enhancement of snowfall rate was simulated in event 3 (e.g., 6%), whereas the highest in event 1 (e.g., 37%). In general, the results provided a comprehensive understanding of how different microphysical processes and environmental conditions influence snowfall characteristics during cloud seeding.

To further understand the impact of different conditions on snow formation, the study involved running the model under four different scenarios, each representing a combination of processes such as diffusion, aggregation, nucleation, and riming. The model was run for Event 1 with various number concentrations ranging from 100 to 1000 cm^{-3} [49] to analyze the sensitivity of cloud microphysics to seeding agent concentration. The left panel in Figure 8 illustrates the evolution of cloud particle number concentration from cloud top to bottom, while the right panel depicts the evolution of snowfall rate for various AgI concentrations of 100 cm^{-3}, 400 cm^{-3}, 700 cm^{-3}, and 1000 cm^{-3} in the seeding plume (lowest 800 m within the cloud layer). The results indicate that higher agent concentrations lead to increased number concentrations and higher snowfall rates because more seeding agents enhance ice crystal formation, which accelerates snowflake growth and increases snowfall. As mentioned in section 2.2, AgI number concentration is assumed to be 700 cm^{-3} throughout the study for main simulations [49]. This concentration was chosen because it effectively promotes ice nucleation and enhances snowfall without excessive use of the seeding agent. The model was then executed with and without accounting for cloud seeding, an important part of our research. This method was intended to assess the impact of cloud seeding on different parameters, including number concentration, IWC, mass-weighted terminal fall speed, and snowfall rate.

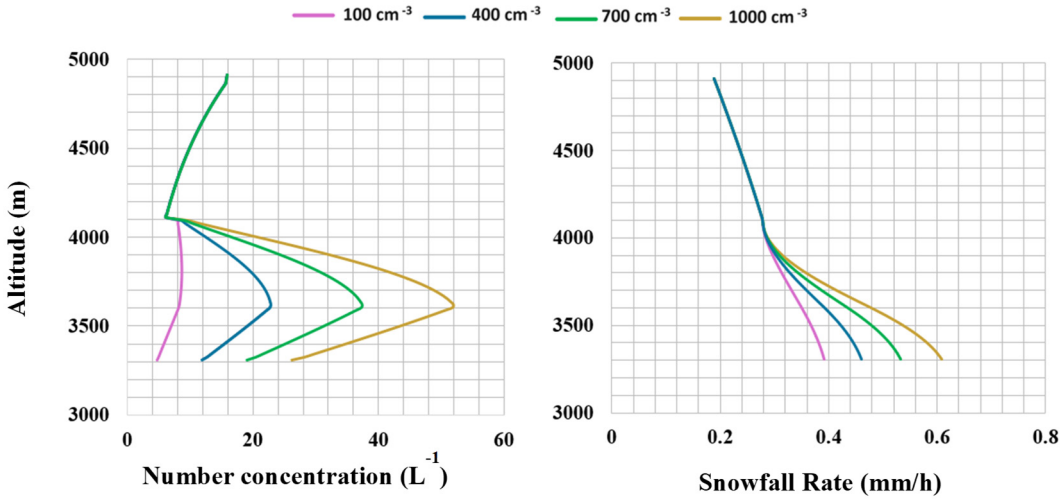

Figure 8. Sensitivity of cloud parameters (cloud particle number concentration and snowfall rate) to AgI Number Concentration (100, 400, 700, 1000 cm^{-3}) with Active Diffusion, Aggregation, Riming, and Nucleation Processes for Event 1.

5. Conclusions

This study presented significant advancements in understanding and modeling cloud seeding as the most common weather modification technique. Deeper insights into the microphysical processes of ice particle growth within seeded clouds were gained through the development and application of the SGMR model. The incorporation of riming and ice nucleation processes into the SGMR allowed for a more accurate simulation of snowfall rate, particularly in the context of cloud-

 doi:10.20944/preprints202410.2154.v1

seeding events in the Tahoe region. Previous studies often lacked a realistic integration of key microphysical processes and did not fully explore their combined effects on precipitation. Additionally, there has been limited research on cloud seeding in the Tahoe area, making this study particularly valuable. This study addresses these gaps by enhancing the SGMR model to incorporate these processes, providing a more comprehensive understanding of cloud seeding's impact on snowfall. Analyzing five varied events in the region, the study found that cloud seeding significantly enhances snowfall rates, increasing them by an average of 24%, with the highest increase being 37%. Seeding also increases the number of ice particles, particularly at lower cloud levels, and enhances IWC through riming. While seeding slightly raises the fall speed of snow particles, the overall impact is minimal due to the small size of nucleated particles. The effectiveness of seeding varies across different events, with the most substantial effects observed in colder, thicker clouds. These enhancements highlighted the potential of cloud seeding to augment precipitation, which was crucial for water resource management, particularly in regions facing water scarcity.

Moreover, the study highlighted the complexities and challenges associated with cloud seeding. Variability in atmospheric conditions and the number concentration of seeding agents were critical factors influencing the outcomes of numerical simulations. These factors significantly affect cloud seeding effectiveness, as insufficient agent concentrations may not enhance precipitation. In addition, high-resolution observational datasets are required to initialize the models and reduce the uncertainty of simulations. While numerical models like the SGMR provided valuable insights, their findings can be validated with in-situ measurements to ensure accuracy. The advancements in modeling and observational capabilities presented were essential for optimizing seeding strategies and maximizing their effectiveness. However, there remains a critical need for more sophisticated mesoscale models that incorporate advanced aerosol schemes and accurately represent cloud and aerosol processes. Such models would allow for a more precise simulation of cloud seeding, accounting for the complex interactions between aerosols, cloud microphysics, and atmospheric dynamics. Incorporating these elements is particularly important in simulating the dispersion and activation of seeding agents like silver iodide, as well as in predicting the resulting changes in cloud properties and precipitation patterns. As climate change and population growth exacerbate water resource challenges, the role of cloud seeding in sustainable water management has become increasingly important. Continued research in weather modification technologies stand crucial for harnessing their full potential to address global water needs.

Author Contributions: Conceptualization, F.H.; methodology, E.E. and F.H.; software, F.H. and E.E.; validation, G.M., F.H., and E.E.; formal analysis, G.M., F.H., and E.E.; investigation, G.M. and F.H.; resources, F.H., F.M., and E.E.; data curation, G.M., F.H., and E.E.; writing—original draft preparation, G.M.; writing—review and editing, G.M. and F.H.; visualization, G.M.; supervision, F.H.; project administration, F.H.; funding acquisition, F.M. and F.H. All authors have read and agreed to the published version of the manuscript.

Funding: This research was supported by Pennington Foundation, grant number 17004.

Institutional Review Board Statement: Not applicable.

Data Availability Statement: The data utilized in this study are publicly available from the following sources: The Modern-Era Retrospective Analysis for Research and Applications, Version 2 (MERRA-2) data, provided by NASA's Global Modeling and Assimilation Office (GMAO), can be accessed at https://gmao.gsfc.nasa.gov/reanalysis/MERRA-2/. The Clouds and the Earth's Radiant Energy System (CERES) data, used to derive cloud and radiation variables, are available through NASA's Atmospheric Science Data Center at https://ceres.larc.nasa.gov/. Those interested in the Snow Growth Model for Rimed Snowfall (SGMR) should reach out the corresponding author.

Acknowledgments: We would like to express our sincere gratitude to Dr. Hosseinpour, the Founder and Director of the DRI's SMART Lab, for her exceptional guidance and significant contribution throughout the research process. Her outstanding expertise and continuous support were crucial to the success of this project. We also wish to thank the anonymous reviewers for their valuable feedback and insights, which improved the quality of this manuscript.

Conflicts of Interest: The authors declare no conflicts of interest.

 doi:10.20944/preprints202410.2154.v1

References

1. Essien, M. (2023). Evaluation of Cloud Seeding Techniques for Precipitation Enhancement. Global Journal of Climate Studies, 1(1), 53-64.
2. Li, D., Zhao, C., Yue, Z., Liu, C., Sun, Y., & Cohen, J. B. (2022). Response of cloud and precipitation properties to seeding at a supercooled cloud-top layer. Earth and Space Science, 9, e2021EA001791. https://doi.org/10.1029/2021EA001791
3. Manton, M. J., L. Warren, S. L. Kenyon, A. D. Peace, S. P. Bilish, and K. Kemsley, 2011: A confirmatory snowfall enhancement project in the Snowy Mountains of Australia. Part I: Project design and response variables. J. Appl. Meteor. Climatol., 50, 1432–1447, https://doi.org/10.1175/2011JAMC2659.1.
4. Manton, M. J., Peace, A. D., Kemsley, K., Kenyon, S., Speirs, J. C., Warren, L., & Denholm, J. (2017). Further analysis of a snowfall enhancement project in the Snowy Mountains of Australia. Atmospheric Research, 193, 192-203.
5. Rasmussen, R. M., Tessendorf, S. A., Xue, L., Weeks, C., Ikeda, K., Landolt, S., Breed, D., Deshler, T., & Lawrence, B. (2018). Evaluation of the Wyoming Weather Modification Pilot Project (WWMPP) Using Two Approaches: Traditional Statistics and Ensemble Modeling. Journal of Applied Meteorology and Climatology, 57(11), 2639-2660. https://doi.org/10.1175/JAMC-D-17-0335.1
6. Ritzman, J. M., Deshler, T., Ikeda, K., & Rasmussen, R. (2015). Estimating the Fraction of Winter Orographic Precipitation Produced under Conditions Meeting the Seeding Criteria for the Wyoming Weather Modification Pilot Project. Journal of Applied Meteorology and Climatology, 54(6), 1202-1215. https://doi.org/10.1175/JAMC-D-14-0163.1
7. Friedrich, K., Ikeda, K., Tessendorf, S. A., French, J. R., Rauber, R. M., Geerts, B., ... & Dawson, N. (2020). Quantifying snowfall from orographic cloud seeding. Proceedings of the National Academy of Sciences, 117(10), 5190-5195.
8. Xue, L. L., Chu, X., Rasmussen, R., Breed, D., Boe, B., & Geerts, B. (2014). The dispersion of silver iodide particles from ground-based generators over complex terrain. Part II: WRF large-eddy simulations versus observations. Journal of Applied Meteorology and Climatology, 53(6),1342–1361. https://doi.org/10.1175/JAMC-D-13-0241.
9. Frencha, J. R., Friedrichb, K., Tessendorfc, S. A., Rauber, R. M., Geerts, B., Rasmussen, R. M., et al. (2018). Precipitation formation from orographic cloud seeding. Proceedings of the National Academy of Sciences of the United States of America, 115(6), 1168–1173. https://doi.org/10.1073/pnas.1716995115
10. Zhao, C., Yang, Y., Fan, H., Huang, J., Fu, Y., Zhang, X., et al. (2020). Aerosol characteristics and impacts on weather and climate over Tibetan Plateau. National Science Review, 7(3), 492–495. https://doi.org/10.1093/nsr/nwz184
11. U.S. Census Bureau, 2010: 2010 Census: Apportionment data. U.S. Census Bureau, https://www.census.gov/data/tables/2010/dec/apportionment-data-text.html.
12. Rauber, R. M., Geerts, B., Xue, L., French, J., Friedrich, K., Rasmussen, R. M., ... & Parkinson, S. (2019). Wintertime orographic cloud seeding—A review. Journal of Applied Meteorology and Climatology, 58(10), 2117-2140.
13. Rasmussen, R., Liu, C., Ikeda, K., Gochis, D., Yates, D., Chen, F., Tewari, M., Barlage, M., Dudhia, J., Yu, W., Miller, K., Arsenault, K., Grubišić, V., Thompson, G., & Gutmann, E. (2011). High-Resolution Coupled Climate Runoff Simulations of Seasonal Snowfall over Colorado: A Process Study of Current and Warmer Climate. Journal of Climate, 24(12), 3015-3048. https://doi.org/10.1175/2010JCLI3985.1
14. Segal, Y., Khain, A., Pinsky, M., & Rosenfeld, D. (2004). Effects of hygroscopic seeding on raindrop formation as seen from simulations using a 2000-bin spectral cloud parcel model. Atmospheric Research, 71(1-2), 3-34.
15. Flossmann, A. I., Manton, M., Abshaev, A., Bruintjes, R., Murakami, M., Prabhakaran, T., & Yao, Z. (2019). Review of advances in precipitation enhancement research. Bulletin of the American Meteorological Society, 100(8), 1465-1480.
16. Laaksonen, A., & Malila, J. (2021). Nucleation of Water: From Fundamental Science to Atmospheric and Additional Applications. Elsevier.
17. Woodley, W. L., Rosenfeld, D., & Silverman, B. A. (2003). Results of on-top glaciogenic cloud seeding in Thailand. Part I: The demonstration experiment. Journal of Applied Meteorology and Climatology, 42(7), 920-938.

18. Maryadi, A., Tomine, K., & Nishiyama, K. (2015). Some aspects of a numerical glaciogenic artificial cloud seeding experiment using liquid carbon dioxide over Kupang, Indonesia. journal of agricultural meteorology, 71(1), 1-14.
19. Tessendorf, S. A., French, J. R., Friedrich, K., Geerts, B., Rauber, R. M., Rasmussen, R. M., ... & Bruintjes, R. (2019). A transformational approach to winter orographic weather modification research: The SNOWIE Project. Bulletin of the American Meteorological Society, 100(1), 71-92.
20. French, J. R., Friedrich, K., Tessendorf, S. A., Rauber, R. M., Geerts, B., Rasmussen, R. M., ... & Blestrud, D. R. (2018). Precipitation formation from orographic cloud seeding. Proceedings of the National Academy of Sciences, 115(6), 1168-1173.
21. Geerts, B., Miao, Q., Yang, Y., Rasmussen, R., & Breed, D. (2010). An airborne profiling radar study of the impact of glaciogenic cloud seeding on snowfall from winter orographic clouds. Journal of the Atmospheric Sciences, 67(10), 3286-3302.
22. Breed, D., Rasmussen, R., Weeks, C., Boe, B., & Deshler, T. (2014). Evaluating winter orographic cloud seeding: design of the Wyoming Weather Modification Pilot Project (WWMPP). Journal of Applied Meteorology and Climatology, 53(2), 282-299.
23. Abshaev, M. T., Abshaev, A. M., Sulakvelidze, G. K., Burtsev, I. I., Malkarova, A. M., & Nesmeyanov, P. A. (2006). Development of rocket and artillery technology for hail suppression. Achievements in weather modification, 109-127.
24. Bruintjes, R. T., Clark, T. L., & Hall, W. D. (1995). The dispersion of tracer plumes in mountainous regions in central Arizona: Comparisons between observations and modeling results. Journal of Applied Meteorology and Climatology, 34(4), 971-988.
25. Xue, L. L., Hashimoto, A., Murakami, M., Rasmussen, R., Tessendorf, S. A., Breed, D., et al. (2013). Implementation of a silver iodide cloud-seeding parameterization in WRF. Part I: Model description and idealized 2D sensitivity tests. Journal of Applied Meteorology and Climatology, 52(6), 1433–1457. https://doi.org/10.1175/JAMC-D-12-0148.1
26. Dessens, J., Sánchez, J. L., Berthet, C., Hermida, L., & Merino, A. (2016). Hail prevention by ground-based silver iodide generators: Results of historical and modern field projects. Atmospheric Research, 170, 98-111.
27. Haupt, S. E., R. M. Rauber, B. Carmichael, J. C. Knievel, and J. L. Cogan, 2018: 100 years of progress in applied meteorology. Part I: Basic applications. A Century of Progress in Atmospheric and Related Sciences: Celebrating the American Meteorological Society Centennial, Meteor. Monogr., No. 59, Amer. Meteor. Soc., https://doi.org/10.1175/AMSMONOGRAPHS-D-18-0004.1.
28. Gabriel, K. R., 1999: Ratio statistics for randomized experiments in precipitation stimulation. J. Appl. Meteor., 38, 290–301, https://doi.org/10.1175/1520-0450(1999)038,0290:RSFREI.2.0.CO;2.
29. Flossmann, A. I., Manton, M., Abshaev, A., Bruintjes, R., Murakami, M., Prabhakaran, T., & Yao, Z. (2018). Peer review report on global precipitation enhancement activities (Research Report). World Meteorological Organization. Retrieved from https://hal.uca.fr/hal-01917801
30. Wang, J., Yue, Z., Rosenfeld, D., Zhang, L., Zhu, Y., Dai, J., ... & Li, J. (2021). The Evolution of an AgI Cloud-Seeding Track in Central China as Seen by a Combination of Radar, Satellite, and Disdrometer Observations. Journal of Geophysical Research: Atmospheres, 126(11), e2020JD033914.
31. Xue, L., Edwards, R., Huggins, A., Lou, X., Rasmussen, R., Tessendorf, S., ... & Parkinson, S. (2017). WRF Large-eddy Simulations of chemical tracer deposition and seeding effect over complex terrain from ground-and aircraft-based AgI generators. Atmospheric Research, 190, 89-103.
32. Xue, L., Chu, X., Rasmussen, R., Breed, D., & Geerts, B. (2016). A Case Study of Radar Observations and WRF LES Simulations of the Impact of Ground-Based Glaciogenic Seeding on Orographic Clouds and Precipitation. Part II: AgI Dispersion and Seeding Signals Simulated by WRF. Journal of Applied Meteorology and Climatology, 55(2), 445-464. https://doi.org/10.1175/JAMC-D-15-0115.1
33. Chu, X., Geerts, B., Xue, L., & Pokharel, B. (2017). A Case Study of Cloud Radar Observations and Large-Eddy Simulations of a Shallow Stratiform Orographic Cloud, and the Impact of Glaciogenic Seeding. Journal of Applied Meteorology and Climatology, 56(5), 1285-1304. https://doi.org/10.1175/JAMC-D-16-0364.1
34. Jing, X., Geerts, B., Wang, Y., & Liu, C. (2017). Evaluating Seasonal Orographic Precipitation in the Interior Western United States Using Gauge Data, Gridded Precipitation Estimates, and a Regional Climate Simulation. Journal of Hydrometeorology, 18(9), 2541-2558. https://doi.org/10.1175/JHM-D-17-0056.1

35. Liu, C., Ikeda, K., Rasmussen, R., Barlage, M., Newman, A. J., Prein, A. F., ... & Yates, D. (2017). Continental-scale convection-permitting modeling of the current and future climate of North America. Climate Dynamics, 49, 71-95.
36. Passarelli, R. E., Jr. (1978): Approximate analytical model of the vapor deposition and aggregation growth of snowflakes, J. Atmos. Sci., 35, 118-124.
37. Mitchell, D. L., Huggins, A., & Grubisic, V. (2006). A new snow growth model with application to radar precipitation estimates. Atmospheric research, 82(1-2), 2-18.
38. Erfani, E. (2016). A Mechanistic Understanding of North American Monsoon and Microphysical Properties of Ice Particles. University of Nevada, Reno.
39. Rienecker, M. M., Suarez, M. J., Gelaro, R., Todling, R., Bacmeister, J., Liu, E., ... & Woollen, J. (2011). MERRA: NASA's modern-era retrospective analysis for research and applications. Journal of climate, 24(14), 3624-3648.
40. Greenwald, T. J., Pierce, R. B., Schaack, T., Otkin, J., Rogal, M., Bah, K., ... & Huang, H. L. (2016). Real-time simulation of the GOES-R ABI for user readiness and product evaluation. Bulletin of the American Meteorological Society, 97(2), 245-261.
41. Gelaro, R., McCarty, W., Suárez, M. J., Todling, R., Molod, A., Takacs, L., ... & Zhao, B. (2017). The modern-era retrospective analysis for research and applications, version 2 (MERRA-2). Journal of climate, 30(14), 5419-5454.
42. Doelling, D. R., Sun, M., Nordeen, M. L., Haney, C. O., Keyes, D. F., & Mlynczak, P. E. (2016). Advances in geostationary-derived longwave fluxes for the CERES synoptic (SYN1deg) product. Journal of Atmospheric and Oceanic Technology, 33(3), 503-521.
43. Wielicki, B. A., Barkstrom, B. R., Harrison, E. F., Lee III, R. B., Smith, G. L., & Cooper, J. E. (1996). Clouds and the Earth's Radiant Energy System (CERES): An earth observing system experiment. Bulletin of the American Meteorological Society, 77(5), 853-868.
44. Loeb, N. G., Su, W., Doelling, D. R., Wong, T., Minnis, P., Thomas, S., & Miller, W. F. (2016). Earth's top-of-atmosphere radiation budget. Reference Module in Earth Systems and Environmental Sciences. ScienceDirect. https://doi.org/10.1016/B978-0-12-409548-9.10367-7
45. Payra, S., Sharma, A., & Verma, S. (2023). Application of remote sensing to study forest fires. In Atmospheric Remote Sensing (pp. 239-260). Elsevier.
46. Justice, C. O., Townshend, J. R. G., Vermote, E. F., Masuoka, E., Wolfe, R. E., Saleous, N., ... & Morisette, J. T. (2002). An overview of MODIS Land data processing and product status. Remote sensing of Environment, 83(1-2), 3-15.
47. Erfani, E., & Mitchell, D. L. (2017). Growth of ice particle mass and projected area during riming. Atmospheric Chemistry and Physics, 17(2), 1241-1257. https://doi.org/10.5194/acp-17-1241-2017
48. Liu, X., Penner, J. E., Ghan, S. J., & Wang, M. (2007). Inclusion of ice microphysics in the NCAR Community Atmospheric Model version 3 (CAM3). Journal of Climate, 20(18), 4526-4547.
49. Marcolli, C., Nagare, B., Welti, A., & Lohmann, U. (2016). Ice nucleation efficiency of AgI: review and new insights. Atmospheric Chemistry and Physics, 16(14), 8915-8937.
50. Achtert, P., O'Connor, E. J., Brooks, I. M., Sotiropoulou, G., Shupe, M. D., Pospichal, B., ... & Tjernström, M. (2020). Properties of Arctic liquid and mixed-phase clouds from shipborne Cloudnet observations during ACSE 2014. Atmospheric Chemistry and Physics, 20(23), 14983-15002.
51. Järvinen, E., Nehlert, F., Xu, G., Waitz, F., Mioche, G., Dupuy, R., … & Schnaiter, M. (2023). Vertical distribution of ice optical and microphysical properties in Arctic low-level mixed-phase clouds during ACLOUD. Atmospheric Chemistry and Physics Discussions, 2023, 1-30.
52. Western Regional Climate Center. Available online: https://wrcc.dri.edu/